

Analytical Formulae for Wind Turbine Tower Loading in the Parked Condition by Using Quasi-Steady Analysis

Nan Xu^{*,1} and Takeshi Ishihara²

¹Research Fellow, Engineering Consulting Department, China Academy of Building Research, 30# Bei San Huan Dong Lu, Beijing, 100013 China.

²Professor, Department of Civil Engineering, The University of Tokyo.

Received 11/2/2013; Revised 21/2/2014; Accepted 21/2/2014

ABSTRACT

The analytical formulae are proposed to estimate the maximum value for along-wind load and across-wind load on the wind turbine towers by using the quasi-steady analysis. The critical parameters in the standard deviation such as the mode correction factors, aerodynamic damping ratios, size reduction factors and wind load ratios are investigated to identify their directional characteristics. A non-Gaussian peak factor is necessary for the along-wind load, while a Gaussian peak factor is acceptable for the across-wind load. A loads combination formula is proposed in order to consider the correlation of along-wind load and across-wind load. The proposed formulae show the favorable agreements with the full dynamic simulation.

Keywords: Quasi-steady analysis, Analytical formulae, Along-wind and across-wind loads, Loads combination, Wind directional characteristics

1. INTRODUCTION

The wind turbines are designed based on the IEC classes, hence, IEC 61400-1 [1] requires the assessment of structural integrity by the load calculations with reference to the site specific conditions. If the turbulent extreme wind model is used, the response shall be estimated using either a full dynamic simulation or a quasi-steady analysis with appropriate corrections for gusts and dynamic response using the formulation in ISO 4354[2] which is applied to the buildings. Wind Energy Handbook[3] adopts the quasi-steady analysis to estimate the wind load on wind turbines in the parked condition, in which the non-linear part of wind load is neglected. Therefore, the wind load may be underestimated for wind turbines exposed to high wind turbulence in mountain areas, since the contribution of non-linear part of wind load is large. Binh et al. [4] considers this non-linear part in the mean wind load and proposes a non-Gaussian peak factor. This model gives a good performance for the prediction of design wind load only in the case that the drag force on rotor is much more dominant than the lift force. In DLC 6.2 the abnormal case (loss of electrical network connection), the wind directions of $-180^{\circ}\sim 180^{\circ}$ should be considered which can cover the yaw misalignment range of $-15^{\circ}\sim 15^{\circ}$ in DLC 6.1 and $-30^{\circ}\sim 30^{\circ}$ in DLC 6.3. In some wind directions, the lift force on rotor may become significant, therefore, the across-wind load should be considered and the combination is necessary.

In this study, the wind load evaluation methods are discussed in Section 2; In Section 3, the analytical formulae for along-wind load and across-wind load are proposed based on quasi-steady analysis, and a loads combination formula is proposed in order to consider the correlation of these two loads. All the proposed formulae are verified by full dynamic simulation, and the characteristics of wind loads are discussed for different size of wind turbines.

2. WIND LOAD EVALUATION METHODS

The wind load on wind turbine is usually evaluated by either a full dynamic simulation or a quasi-steady analysis. While the full dynamic simulation is commonly used in the turbine design, the quasi-steady

*Corresponding Author: Fax:+86-84279246, E-mail:nanxu08@sina.com

analysis is used widely in the design of tower and other support structures. Quasi-steady analysis is adopted in many design codes (AIJ [5]; DS472 [6]). This study will investigate the quasi-steady analysis to estimate the wind load and use the full dynamic simulation as the validation.

2.1. Quasi-steady analysis

In quasi-steady analysis, a coefficient called peak factor proposed by Davenport [7] to account for fluctuating wind load is used. The maximum bending moment is estimated by eqn (1).

$$M_D(z) = \overline{M}_D(z) + \sigma_{MD}(z) \cdot g_D, \quad M_L(z) = \overline{M}_L(z) + \sigma_{ML}(z) \cdot g_L \quad (1)$$

where \overline{M}_{Df} is the mean bending moment, σ_{Mf} is the standard deviation, g_f is the peak factor. The wind direction and wind load on wind turbine are defined as Fig. 1.

The assumptions used in this study are listed below:

- 1) Mean wind velocity U_h and turbulence intensity I_h at the hub height are used as representative for that of the whole rotor; while the mean wind velocity profile $U(z) = U_h (z/H_h)^\alpha$ and turbulence intensity profile $I_u(z) = I_h (z/H_h)^{-\alpha-0.05}$ are considered for tower, where z is the height to the ground, H_h is the hub height, and α is the exponent of the wind profile.
- 2) The equivalent aerodynamic coefficients for the whole rotor are used instead of that varying with positions on the rotor, which is discussed in *Section 2.4*.
- 3) The model of an elastic tower and a rigid rotor, shown in Fig. 2b, is used to implement the theoretical formula of wind load. The tower height is assumed to be equal to the hub height, and the rotor part of this study includes blades, hub and nacelle; Since in wind load of wind turbine tower the effect of the first mode is dominant, only the first mode is considered. Referring to Ishihara [8] the first mode shape for rotor is assumed as $\mu_1 = 1$ and $\mu_1(z) = (z/H_h)^{\beta_s}$ is used for tower, where $\beta_s = 2.0$ (Zhu [9]); Structural damping ratios of the first mode $\xi_s = c_1/4\pi m_1 n_1$ are assumed to be equal in the along-wind and across-wind vibrations, and $\xi_s = 0.8\%$ is used in this study for the wind turbines with gear box (Ishihara et al. [10]).
- 4) The mean bending moment is derived as the function of height on the tower as well as the standard deviation, whose variation with height only depends on the mean bending moment, since their ratio is found to be almost constant along the tower from the full dynamic simulation, which means all the other parameters in standard deviation can be considered constant along the tower, and proposed based on the integration of the whole wind turbine. The peak factor is proposed considering the response of the whole wind turbine [4], so it doesn't change with height either. This bending moment-based peak factor can be used for the calculation of shear force on the wind turbine tower.
- 5) Since the bending moment is dominant for the buckling of the tower [10], the estimation of shear force is not presented in this paper. This study discusses the wind-induced bending

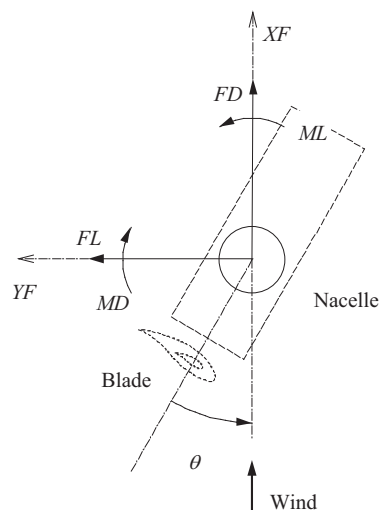


Figure 1. Wind direction and wind load

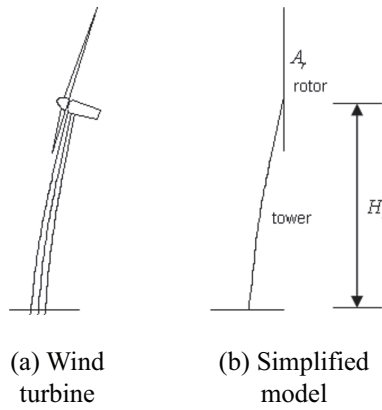


Figure 2. Wind turbine and simplified model

moment, therefore, the bending moment due to the gravity of the rotor and nacelle is not added here, however, it should be taken into account in the real design. It is noted that this study is used for the commercial wind turbine with tubular tower.

Considering a wind with longitudinal fluctuating component u and lateral fluctuating component v , the relation between wind velocity and a vibrated element in two-dimensional direction under wind direction θ is shown in Fig. 3. Quasi-static method is used to calculate the wind force. By using the following assumptions:

- 1) Make Taylor expansion around $\theta = 0$, and note $\theta \approx \tan\theta = (v-\dot{y})/(U+u-\dot{x})$ since θ is very small;
- 2) Drop the second order terms by perturbation analysis, but keep the term $(1/2) \rho c A_f(\theta) u^2$ since the contribution of this non-linear part of wind force is large, especially for high wind turbulence (Binh et al. [4]);
- 3) Remove the terms caused by the across motion of the structure which cannot be obtained by the analytical method;

The total drag force F_D and lift force F_L can be expressed as following:

$$F_D = \frac{1}{2} \rho c(r) C_D(\theta) U^2 + \frac{1}{2} \rho c(r) C_D(\theta) u^2 + \rho c(r) C_D(\theta) Uu + \rho c(r) A_D(\theta) Uv - \rho c(r) C_D(\theta) U\dot{x} \tag{2}$$

$$F_L = \frac{1}{2} \rho c(r) C_L(\theta) U^2 + \frac{1}{2} \rho c(r) C_L(\theta) u^2 + \rho c(r) C_L(\theta) Uu + \rho c(r) A_L(\theta) Uv - \rho c(r) A_L(\theta) U\dot{y} \tag{3}$$

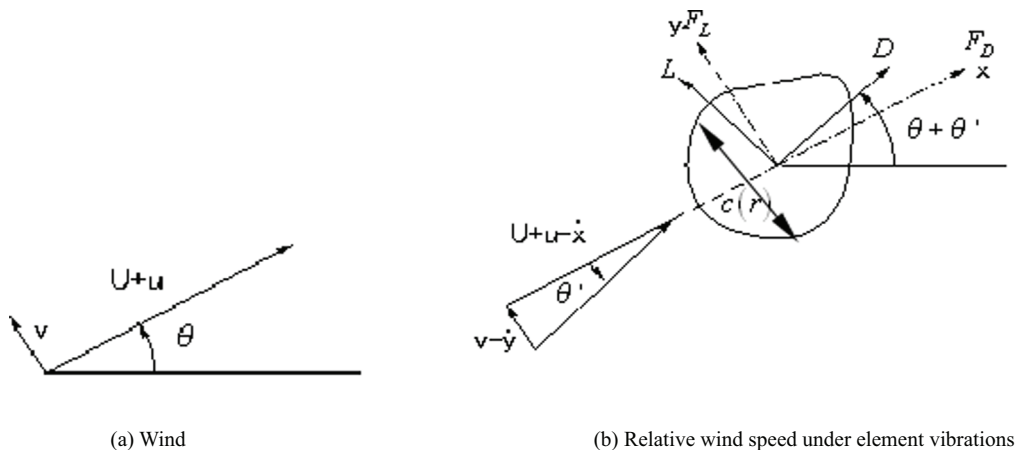


Figure 3. Relation between wind and a vibrated element

where ρ is the air density, $c(r)$ is the characteristic length of the element at position r , U is the mean wind velocity, $C_D(\theta)$ and $C_L(\theta)$ are the drag and lift aerodynamic coefficients respectively, $A_D(\theta) = 0.5(\partial C_D(\theta)/\partial\theta - C_L(\theta))$ and $A_L(\theta) = 0.5(C_D(\theta) + \partial C_L(\theta)/\partial\theta)$ are the aerodynamic coefficient gradients for along-wind and across-wind loads respectively, and are the along-wind and across-wind structural vibration velocity, respectively.

2.2. Full dynamic simulation

The full dynamic simulation code named CA τ T (Computer-Aided Aerodynamic and Aeroelastic Technology), which developed by the Bridge & Structure laboratory group in University of Tokyo, Japan (Ishihara et al.[10]), is used for dynamic response analysis for wind turbines to the three dimensional turbulent wind fields. CA τ T does not use a modal superposition solution to the dynamic equations like the common commercial aeroelastic codes for wind turbines, but instead directly solves the equations of motion for a given arbitrary set of forces acting on the structure and for forces generated by the structure itself at each time step based on an aeroelastic calculation procedure, as detailed in Table 1. This code has been verified by field test. The general formulation of the differential equation of motion for the structure is given at eqn (4):

$$[M]\ddot{x} + [C]\dot{x} + [K]x = [F] \quad (4)$$

where $[M]$ is the mass matrix, $[C]$ is the damping matrix, $[K]$ is the stiffness matrix, $[F]$ is the external force matrix.

2.3. Wind turbine model

Seven 3-blade wind turbine models of 100kW~2000kW are used in this study to investigate the tower wind load. The first natural frequency and mode shape are obtained by eigenvalue analysis. From the eigenvalue analysis, the first mode shape for rotor can be assumed as $\mu_1 = 1$ and $\mu_1(z) = (z/H_h)^{\beta_s}$ is proposed for tower, where $\beta_s = 2.0$ (Zhu[9]). The main information of each wind turbine is described in Table 2.

Table 1. Description of the full dynamic simulation code CA τ T

Name	Description
Eigenvalue analysis	Subspace iteration procedure
Dynamic analysis	Direct numerical integration, Newmark- β method
Element type	Beam element (12-DOF)
Formulation	Total Lagrangian formulation
Damping estimation	Rayleigh damping model
Aerodynamic force	Quasi-steady aerodynamic theory

Table 2. Wind turbine description

Name	Description						
Rated power (kW)	100	400	500	600	1000	1500	2000
Rotor radius R (m)	11.8	15.5	20.2	25.8	32.5	38.3	40.7
Hub height H_h (m)	24.0	36.0	44.0	50.0	70.0	69.0	76.5
1st frequency n_1 (Hz)	2.03	0.81	0.50	0.53	0.41	0.43	0.49
Rotor mass m_r (kg)	13000	17800	29650	37903	76610	89400	105641
Tower mass m_f (kg)	16700	20910	36089	41233	109400	108390	143287
1st modal mass m_1 (kg)	15551	21250	33538	42868	89237	100756	123461

2.4. Equivalent aerodynamic coefficients for rotor

The equivalent drag and lift aerodynamic coefficients $C_{D,r}(\theta)$ and $C_{L,r}(\theta)$ for rotor are defined as:

$$C_{D,r}(\theta) = \left(C_{D,n}(\theta)A_n + 3\int_0^R C_{D,b}(r,\theta)c(r)dr \right) / A_r \tag{5}$$

$$C_{L,r}(\theta) = \left(C_{L,n}(\theta)A_n + 3\int_0^R C_{L,b}(r,\theta)c(r)dr \right) / A_r \tag{6}$$

where $A_n = L_n H_n + (\pi/4)R_n H_n$ is wind-acting area of hub and nacelle, illustrated in Fig. 4; A_r is the rotor area, including the blades, hub and nacelle; $C_{D,n}$ and $C_{L,n}$ are drag and lift aerodynamic coefficients of nacelle (Fig. 5a); $C_{D,b}$ and $C_{L,b}$ are drag and lift aerodynamic coefficients of blade, which depend on the thickness ratio (thickness/chord) of the blade section. 2M wind turbine blade section (thickness ratio: 12%) by GH Bladed[11] and s809 (thickness ratio: 21%) by Somers[12], will be considered (Fig. 5b). Fig. 6 illustrates the variation of equivalent drag and lift aerodynamic coefficients of rotor as well, which strongly correlates with those of blade, where $C_{D,r}(\theta)$ shows minimum near $\pm 90^\circ$ and maximum near 0° and $\pm 180^\circ$, while $C_{L,r}(\theta)$ becomes 0 near $\pm 180^\circ$, 0° and $\pm 90^\circ$.

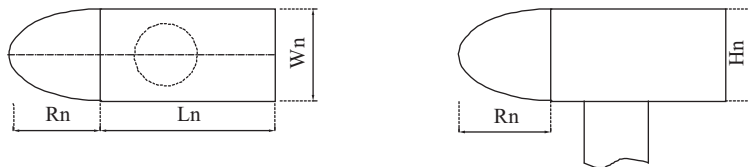


Figure 4. Configuration of nacelle and hub

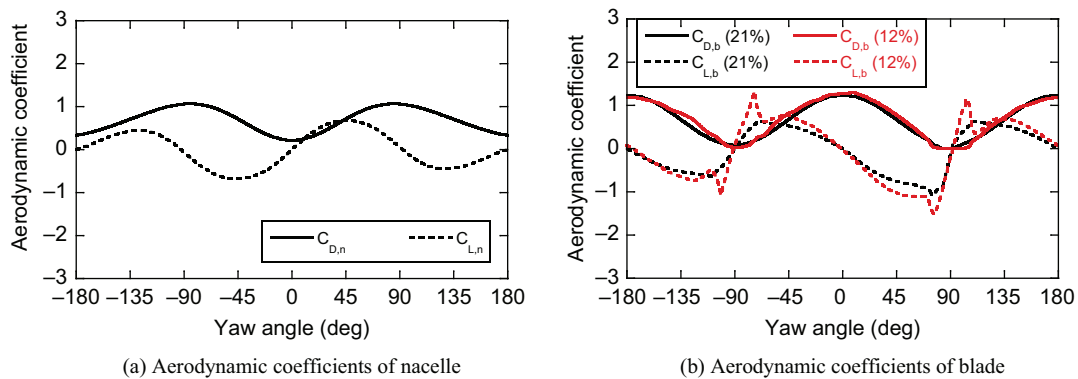


Figure 5. Aerodynamic coefficients for nacelle and blade

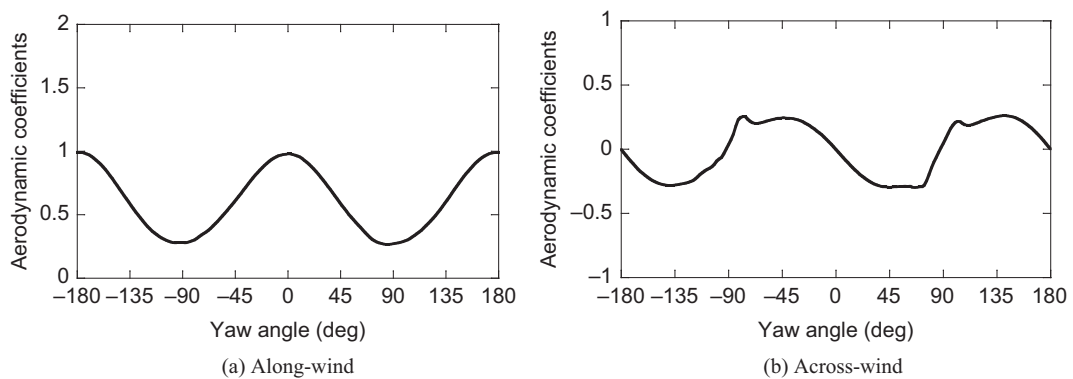


Figure 6. Equivalent aerodynamic coefficients for rotor (400kW)

3. WIND LOAD EVALUATION

The integral forms of mean value, standard deviation and peak factor of bending moment are derived[8]. The analytical formulae are proposed in this study to make them easily applied for the estimation of wind load by engineers and get a clear understanding of the characteristics for each parameter as well (*Sections 3.1, 3.2, and 3.3, respectively*). In standard deviation (*Sections 3.2*), the mode correction factor, aerodynamic damping ratio, size reduction factor and wind load ratio are investigated to identify their directional characteristics. In *Section 3.4*, the loads combination formula is proposed in order to consider the correlation of along-wind load and across-wind load.

3.1. Mean bending moment

Binh et al. [4] considers the non-linear part in the mean wind load. This model gives a good performance only for the prediction of along-wind load and it is integral form. This study proposes the analytical formulae for not only along-wind but also across-wind mean bending moments.

From eqns (2-3), the mean wind force \bar{F}_D and \bar{F}_L are derived as:

$$\bar{F}_D = \frac{1}{2} \rho C_D(\theta) c(r) (U^2 + \sigma_u^2) = \frac{1}{2} \rho C_D(\theta) c(r) U^2 (1 + I_u^2) \quad (7)$$

$$\bar{F}_L = \frac{1}{2} \rho C_L(\theta) c(r) (U^2 + \sigma_u^2) = \frac{1}{2} \rho C_L(\theta) c(r) U^2 (1 + I_u^2) \quad (8)$$

Then the mean bending moment \bar{M}_D , \bar{M}_L can be easily derived as eqns (9-10). By considering the loads for rotor and tower separately, taking the mean wind velocity and turbulence intensity of hub as representative for that of the whole rotor, and applying equivalent aerodynamic coefficients for the rotor, the simplified formulae of \bar{M}_D and \bar{M}_L are proposed as well.

$$\begin{aligned} \bar{M}_D(z) &= \int_z \frac{1}{2} \rho C_D(r, \theta) c(r) U^2(r) [1 + I_u^2(r)] r dr \\ &\approx \frac{1}{2} \rho U_h^2 [C_{D,r}(\theta) (1 + I_{uh}^2) A_r (H_h - z) + C_{D,t} H_h^2 D'] \end{aligned} \quad (9)$$

$$\begin{aligned} \bar{M}_L(z) &= \int_z \frac{1}{2} \rho C_L(r, \theta) c(r) U^2(r) [1 + I_u^2(r)] r dr \\ &\approx \frac{1}{2} \rho U_h^2 C_{L,r}(\theta) (1 + I_{uh}^2) A_r (H_h - z) \end{aligned} \quad (10)$$

where

$$\begin{aligned} D' &= \frac{D_b}{2\alpha + 2} \left(1 - \left(\frac{z}{H_h} \right)^{2\alpha+2} \right) - \frac{D_b - D_t}{2\alpha + 3} \left(1 - \left(\frac{z}{H_h} \right)^{2\alpha+3} \right) \\ &\quad + \frac{I_{uh}^2 D_b}{1.9} \left(1 - \left(\frac{z}{H_h} \right)^{1.9} \right) - \frac{I_{uh}^2 (D_b - D_t)}{2.9} \left(1 - \left(\frac{z}{H_h} \right)^{2.9} \right) \end{aligned}$$

I_{uh} is the along-wind turbulence intensity at hub height; D_b and D_t are the diameter of the bottom and top of tower; $C_{D,t}$ and $C_{L,t}$ are the drag and lift aerodynamic coefficients of cylindrical tower, respectively, which are regarded to be constant. Referring to BSI code[13], $C_{D,t} = 0.6$ and $C_{L,t} = 0$ are used in this study. From eqn (9), it is found that the along-wind mean bending moment is the summation of those from rotor and tower, while for across-wind load, since $C_{L,t}(\theta) = 0$, only rotor contributes to the mean bending moment (eqn (10)), and becomes 0 at some yaw angles.

With 400kW wind turbine, $U_h = 50\text{m/s}$ and $I_{uh} = 0.158$ the proposed formulae for mean bending moment are verified for different yaw angles and different heights on tower by full dynamic simulation, as shown in Figs. 7 and 8.

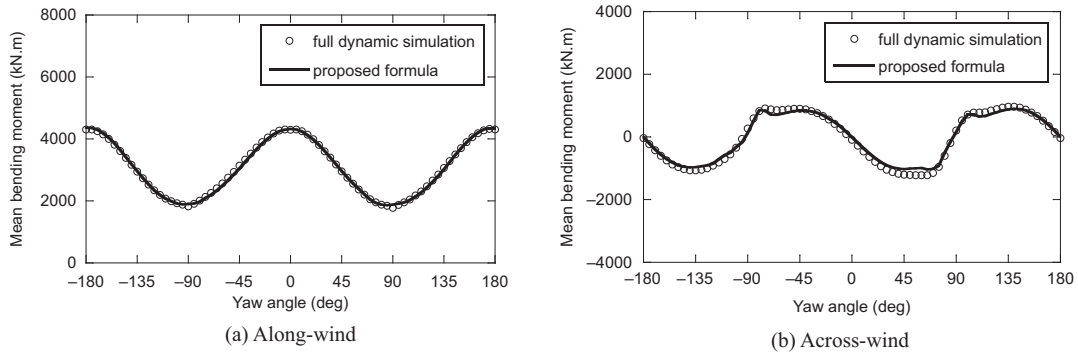


Figure 7. Comparison of tower base mean bending moment for different yaw angles

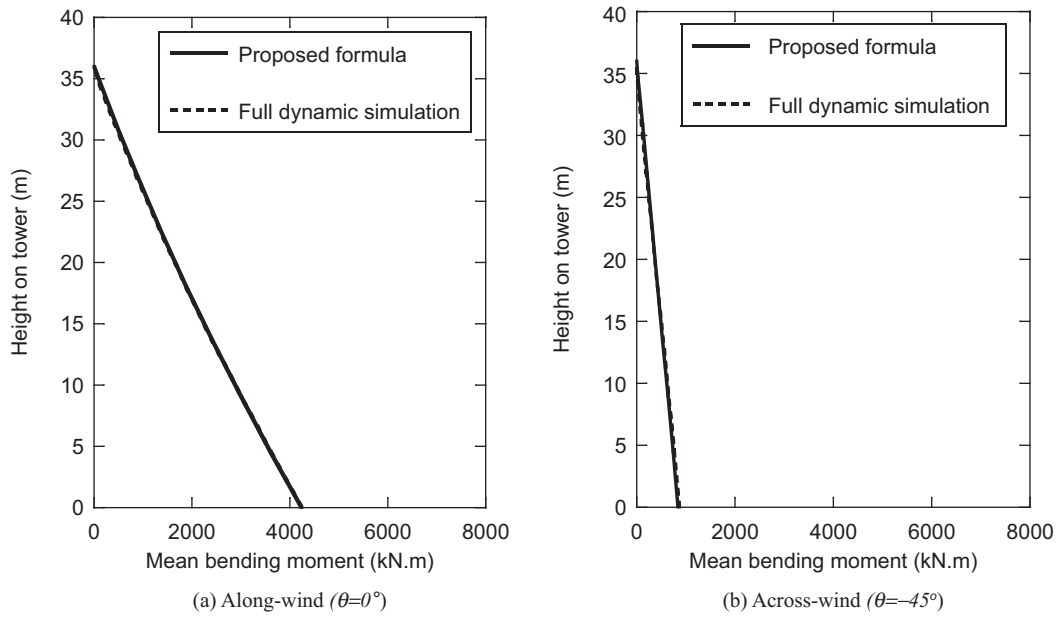


Figure 8. Comparison of mean bending moment for different heights on tower

3.2. Standard deviation

The analytical formulae for standard deviation are proposed in this study from the integral forms in order to get a clear understanding whether the mode correction factors, aerodynamic damping ratios, size reduction factors and wind load ratios depend on the yaw angle or not.

The fluctuating wind force q_D and q_L can be obtained by removing the mean wind force \bar{F}_D and \bar{F}_L from the total force F_D and F_L , respectively. Since the non-linear parts in q_D and q_L contribute very little to the standard deviation of bending moment compared to linear parts, in this paper only linear parts are used in the theoretical derivation. Therefore, the fluctuating wind force per unit length on wind turbine for along-wind response and across-wind response is finally determined as:

$$q_D(r,t) = [\rho c(r)C_D(\theta)Uu + \rho c(r)A_D(\theta)Uv] - \rho c(r)C_D(\theta)U\dot{x} \tag{11}$$

$$q_L(r,t) = [\rho c(r)C_L(\theta)Uu + \rho c(r)A_L(\theta)Uv] - \rho c(r)A_L(\theta)U\dot{y} \tag{12}$$

It is derived that the standard deviation of fluctuating wind load consists of a background part and a resonant part as shown in eqn (13) based on eqns (11-12). The resonant one can be derived by means of modal analysis, as shown in eqn (A.7). All the detailed derivation of standard deviation is given in *Appendix*.

$$\sigma_{MD}(z) = \sqrt{\sigma_{MBD}^2(z) + \sigma_{MRD}^2(z)}, \quad \sigma_{ML}(z) = \sqrt{\sigma_{MBL}^2(z) + \sigma_{MRL}^2(z)} \quad (13)$$

For wind turbine, the across-wind mean bending moment becomes close to zero at some yaw angles. In this study the along-wind mean bending moment \overline{M}_D is employed to calculate both along-wind and across-wind standard deviation of bending moment. The background standard deviation should include two components σ_{MBDu} , σ_{MBDv} or σ_{MBLu} , σ_{MBLv} , which depend on the fluctuation component u and v , respectively, as well as the resonant standard deviation which consists of σ_{MRDu} , σ_{MRDv} or σ_{MRLu} , σ_{MRLv} . All these components are summarized in Table 3.

Table 3. Components of standard deviation

Name	Along-wind	Across-wind
Background	$\sigma_{MBD}(z) = \sqrt{\sigma_{MBDu}^2(z) + \sigma_{MBDv}^2(z)}$	$\sigma_{MBL}(z) = \sqrt{\sigma_{MBLu}^2(z) + \sigma_{MBLv}^2(z)}$
	where	where
	$\sigma_{MBDu}(z) = 2 \frac{\overline{M}_D(z)}{1 + I_{uh}^2} I_{uh} \sqrt{K_{MBDu} \cdot \gamma_{MBDu}}$	$\sigma_{MBLu}(z) = 2 \frac{\overline{M}_D(z)}{1 + I_{uh}^2} I_{uh} \sqrt{K_{MBLu} \cdot \gamma_{MBLu}}$
	$\sigma_{MBDv}(z) = 2 \frac{\overline{M}_D(z)}{1 + I_{vh}^2} I_{vh} \sqrt{K_{MBDv} \cdot \gamma_{MBDv}}$	$\sigma_{MBLv}(z) = 2 \frac{\overline{M}_D(z)}{1 + I_{vh}^2} I_{vh} \sqrt{K_{MBLv} \cdot \gamma_{MBLv}}$
Resonant	$\sigma_{MRD}(z) = \sqrt{\sigma_{MRDu}^2(z) + \sigma_{MRDv}^2(z)}$	$\sigma_{MRL}(z) = \sqrt{\sigma_{MRLu}^2(z) + \sigma_{MRLv}^2(z)}$
	where	where
	$\sigma_{MRDu}(z) = 2 \frac{\overline{M}_D(z)}{1 + I_{uh}^2} \frac{I_{uh} \pi \phi_D}{\sqrt{4\pi\xi_D}} \sqrt{R_{uh}(n_1)}$	$\sigma_{MRLu}(z) = \frac{2\overline{M}_D(z)}{1 + I_{uh}^2} \frac{I_{uh} \pi \phi_L}{\sqrt{4\pi\xi_L}} \sqrt{R_{uh}(n_1)}$
	$\sigma_{MRDv}(z) = 2 \frac{\overline{M}_D(z)}{1 + I_{vh}^2} \frac{I_{vh} \pi \phi_D}{\sqrt{4\pi\xi_D}} \sqrt{R_{vh}(n_1)}$	$\sigma_{MRLv}(z) = \frac{2\overline{M}_D(z)}{1 + I_{vh}^2} \frac{I_{vh} \pi \phi_L}{\sqrt{4\pi\xi_L}} \sqrt{R_{vh}(n_1)}$

ϕ_D , ϕ_L are the mode correction factor, ξ_D and ξ_L are the damping ratio, K_{MBDu} , K_{MBDv} and, K_{MRDu} (n_1), K_{MRDv} (n_1) are denoted the background and resonant size reduction factors of along-wind load owing to the lack of correlation of longitudinal and lateral wind fluctuations, K_{MRLu} , K_{MRLv} and K_{MELu} (n_1), K_{MELv} (n_1) are the background and resonant size reduction factors of across-wind load, n_1 is the first modal frequency of the tower, $I_{vh} = 0.8 I_{uh}$ is the across-wind turbulence intensity at hub height, $R_{uh}(n_1)$ and $R_{vh}(n_1)$ are the normalized Von Karman power spectral density of longitudinal and lateral wind fluctuation[14], γ_{MBDu} , γ_{MBDv} , γ_{MRDu} , γ_{MRDv} , γ_{MRLu} , γ_{MRLv} , γ_{MELu} , γ_{MELv} are the wind load ratios, which can be considered as the correction factors of the size reduction factors due to the employing of along-wind mean bending moment to calculate the standard deviation of bending moment.

3.2.1. Mode correction factors

Resulted from the employing of along-wind mean bending moment M_D to calculate the standard deviation of bending moment, the same mode correction factor can be used for along-wind and across-wind. Through theoretical derivation, finally the integral form of mode correction factors can be expressed as eqn (14):

$$\phi_D = \phi_L = \frac{\int C_D(r, \theta) \mu_1(r) c(r) dr}{\int C_D(r, \theta) c(r) r dr} \frac{\int m(r) \mu_1(r) r dr}{m_1} \approx \frac{m_s}{m_1} \cdot \left(\frac{\gamma_m / a' + 1}{\gamma_m + 1} \cdot a' \right) \cdot \left(\frac{\gamma_F / b' + 1}{\gamma_F + 1} \cdot b' \right) \quad (14)$$

where

$$\gamma_m = \frac{m_r}{m_t}, \quad \gamma_F = \frac{C_{D,r}(\theta)A_r}{\int_0^{H_h} C_{D,t}(\theta)d(z)\frac{z}{H_h} dz} = \frac{C_{D,r}(\theta)A_r}{C_{D,t}(\theta)\cdot 0.42D_a H_h},$$

$$a' = \frac{\int_0^{H_h} m(z)\mu_1(z)z dz}{m_t H_h} = \frac{\int_0^{H_h} m\left(\frac{z}{H_h}\right)^{\beta_s} z dz}{m H_h \cdot H_h} = \frac{1}{2 + \beta_s}.$$

$$b' = \frac{\int_0^{H_h} C_{D,t}(\theta)d(z)\mu_1(z) dz}{\int_0^{H_h} C_{D,t}(\theta)d(z)\frac{z}{H_h} dz} \approx \frac{C_{D,t}(\theta)\cdot 0.3D_a H_h}{C_{D,t}(\theta)\cdot 0.42D_a H_h}.$$

$m(r)$ is the mass per length of the element at position r . m_s is the total mass of wind turbine. m_1 is the generalized mass of the whole wind turbine for the first mode. $d(z) = D_b - (D_b - D_t)z/H_h$ is the diameter of tower. m_r and m_t are the mass of rotor and tower, respectively. γ_m is rotor-tower ratio of mass, which changes very little for different wind turbines with an average of 0.80 referring to Table 2. γ_F is rotor-tower ratio of load, which varies with yaw angle. α' is derived theoretically, assuming uniform mass distribution which is m per unit length along the tower, and the expression is the same as that given by AIJ[5]. With $\beta_s = 2.0$ (Zhu[9]), $\alpha' = 0.25$ is proposed. b' is derived theoretically and its approximate value of 0.714 is very close to $1 - 0.4 \ln \beta_s$ which is given by AIJ[5]. All the parameters in the formula of mode correction factor are listed in Table 4.

A unified mode correction factor is obtained for different wind turbines. Fig. 9 shows good agreement between the proposed formula and the integral form. Due to the existence of rotor, ϕ_D and ϕ_L vary with yaw angle in a range larger than that of tower. In the mode correction factor, γ_m and γ_F can be considered as the factors which indicate the rotor effect on tower. It is noticed that if the rotor is removed, $\gamma_m = \gamma_F = 0$, which will make the mode correction factor the same as that given in AIJ[5] for towers or high-rise buildings.

Table 4. Parameters in the formula of mode correction factor

Parameters	γ_m	γ_F	a'	b'
Proposed value	0.80	$\frac{C_{D,r}(\theta)A_r}{C_{D,t}(\theta)\cdot 0.42D_a H_h}$	0.25	0.714

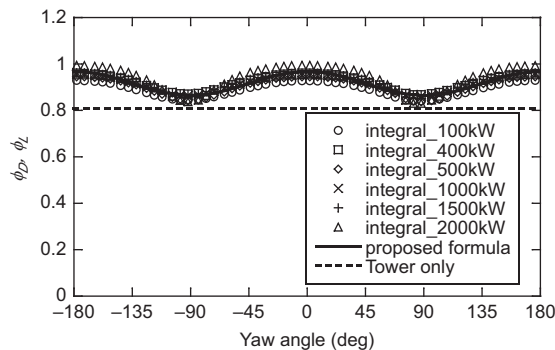


Fig. 9. Comparison of mode correction factors

3.2.2. Aerodynamic damping ratios

From eqn (A.7), in the case of the dominant first mode, the total damping ratio should be the summation of structural damping ratio ξ_s and aerodynamic damping ratio ξ_{aD} or ξ_{aL} . Due to the

existence of rotor, the aerodynamic damping may become much larger than the structural one at some wind direction and cannot be neglected, which is different from the high-rise buildings and chimneys. It should be noted that for across-wind load, since the aerodynamic damping ratio ξ_{aL} may become negative at some yaw angle $\xi_L = \max(\xi_s + \xi_{aL}, \xi_s)$ is used to limit the total damping ratio ξ_L not less than the structural one in order to avert aero-elastic instability.

For along-wind load, the aerodynamic damping ratio ξ_{ad} contains two parts: the aerodynamic damping ratio for the rotor and the tower, as expressed in eqn (15). It is found that most of the aerodynamic damping of wind turbine comes from the rotor, which results in nearly 9 times of that from the tower at most. While for across-wind load, since the aerodynamic coefficient gradient $A_{L,r}(\theta) = 0$ for tower, the aerodynamic damping ratio ξ_{aL} is totally caused by rotor, as expressed in eqn (16). Both ξ_{ad} and ξ_{aL} are the functions of yaw angle.

$$\xi_{ad} = \frac{\int \rho C_D(r, \theta) U(r) c(r) \mu_1^2(r) dr}{4\pi m_1 n_1} = \frac{\rho U_h}{4\pi m_1 n_1} (C_{D,r}(\theta) A_r + C_{D,t}(\theta) H_h D'') \quad (15)$$

$$\xi_{aL} = \frac{\int \rho A_L(r, \theta) U(r) c(r) \mu^2(r) dr}{4\pi m_1 n_1} = \frac{\rho U_h A_r A_{L,r}(\theta)}{4\pi m_1 n_1} \quad (16)$$

where

$$D'' = \frac{D_b + (\alpha + 5) D_t}{(\alpha + 5)(\alpha + 6)}, \quad A_{L,r}(\theta) = 3 \int_0^R \frac{1}{2} \left(C_{D,b}(r, \theta) + \frac{\partial C_{L,b}}{\partial \theta}(r, \theta) \right) c(r) dr / A_r.$$

$A_{L,r}(\theta)$ is the equivalent aerodynamic coefficient gradient of rotor.

3.2.3. Size reduction factors

The integral forms of all the background and resonant size reduction factors are shown in *Appendix*. From the integral calculation, it is found that all the size reduction factors are almost constant with different yaw angles, since the aerodynamic coefficients in the numerator and denominator of the integral forms can eliminate each other much. Hence, it can be assumed that they don't vary with yaw angle. In addition, it can be observed from the integral form that the background size reduction factor should be a function of the turbulence integral length scale L_u or L_v ($L_v = 0.33 L_u$ is for the across-wind load) and the rotor radius R which is taken as the characteristic size of the whole wind turbine in this study. Referring to AIJ [5], the formula format for lattice structures, $1/(1 + \beta_B \cdot R/0.3L_u)$ or $1/(1 + \beta_B \cdot R/0.3L_v)$ is adopted here. While the resonant size reduction factor should be a function of the non-dimensional decay factor C (Cramer[15], indicated values of C ranging from 7 to 50, so $C = 8.0$ is used here), the first modal natural frequency n_1 , rotor radius R , and mean wind speed at hub height U_h , then the formula format becomes $1/(1 + \beta_R \cdot C_{n1} R / U_h)^2$. The unknown factors β_B and β_R can be identified by fitting the results from the integral form of seven different sizes of wind turbines. For each wind turbine, the mean value of different yaw angles is taken as the result of the integral form. Finally, the formulae of background and resonant size reduction factors for along-wind and across-wind standard deviation are proposed as Table 5.

Fig. 10 shows good agreement between the proposed formula and the integral form for each size reduction factor. Both background and resonant size reduction factors vary in the range of 0 ~ 1.0, and the background one decreases when the wind turbine size increases. However, the resonant one doesn't have this feature, since it is also related to the natural frequency of wind turbine. Since L_v is smaller than L_u , K_{MBL_v} is smaller than K_{MBL_u} , which indicates that the smaller turbulence integral length scale results in the more lack of correlation of the fluctuating wind velocity and the size effect becomes more significant.

3.2.4. Wind load ratios

Wind load ratios can be considered as the correction factors of the size reduction factors. They are resulted from the employing of along-wind mean bending moment M_D to calculate the standard deviation of bending moment. By considering the wind load ratios from rotor and tower separately, the formulae of background and resonant wind load ratios for along-wind and across-wind

Table 5. Proposed formulae for size reduction factors

Name	Along-wind	Across-wind
Background	$K_{MBDu} = \frac{1}{1 + 0.69 \frac{R}{0.3L_u}}$	$K_{MBLu} = \frac{1}{1 + 0.5 \frac{R}{0.3L_u}}$
	$K_{MBDv} = \frac{1}{1 + 0.69 \frac{R}{0.3L_v}}$	$K_{MBLv} = \frac{1}{1 + 0.5 \frac{R}{0.3L_v}}$
Resonant	$K_{MRDu}(n_1) = K_{MRDv}(n_1) = \frac{1}{\left(1 + 0.26 \frac{Cn_1 R}{U_h}\right)^2}$	$K_{MRLu}(n_1) = K_{MRLv}(n_1) = \frac{1}{\left(1 + 0.21 \frac{Cn_1 R}{U_h}\right)^2}$

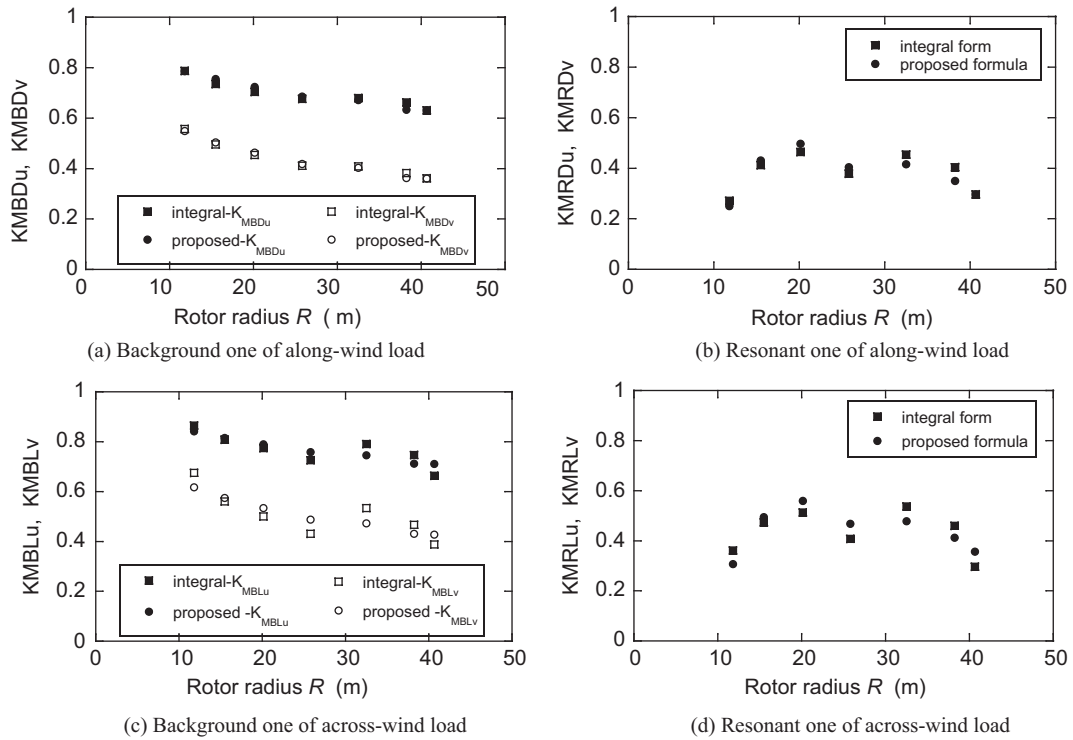


Figure 10. Variation of size reduction factors with rotor radius

standard deviation are proposed as Table 6 from their integral forms which are presented in Appendix.

where $a_B = A_r/C_{D,i}(\theta) \cdot 0.47D_aH_h$ and $a_R = A_r/C_{D,i}(\theta) \cdot 0.3D_aH_h$ are the rotor-tower ratios of area for background and resonant response, respectively, and $D_a = (D_b + D_t)/2$ is the average diameter of tower. It is noticed from the proposed formulae that the wind load ratios are 1 or close to 0 for along-wind load, while they are the functions of yaw angle for across-wind load. By full dynamic simulation, it is found that for along-wind load the standard deviation σ_{MBDv} and σ_{MRDv} due to lateral wind fluctuation v can be neglected compared to σ_{MBDu} and σ_{MRDu} due to longitudinal wind fluctuation u , as shown in Fig. 11a, which is resulted from that γ_{MBDv} and γ_{MRDv} are close to 0 in Table 6. While for across-wind load in both background and resonant standard deviation σ_{MBL} and σ_{MRL} , neither part caused by the two wind fluctuation components can be neglected, since u contributes a lot to the standard deviation as well, although around the 0° and $\pm 90^\circ$ most of the standard deviation comes from v , as shown in Fig. 11b.

Table 6. Wind load ratios

Name	Along-wind	Across-wind
Background	$\gamma_{MBDu} = 1$ $\gamma_{MBDv} \approx 0$	$\gamma_{MBLu} = \left(\frac{C_{L,r}(\theta) \cdot a_B}{1 + C_{D,r}(\theta) \cdot a_B} \right)^2$, $\gamma_{MBLv} = \left(\frac{A_{L,r}(\theta) \cdot a_B}{1 + C_{D,r}(\theta) \cdot a_B} \right)^2$
Resonant	$\gamma_{MRDu} = 1$ $\gamma_{MRDv} \approx 0$	$\gamma_{MRLu} = \left(\frac{C_{L,r}(\theta) \cdot a_R}{1 + C_{D,r}(\theta) \cdot a_R} \right)^2$, $\gamma_{MRLv} = \left(\frac{A_{L,r}(\theta) \cdot a_R}{1 + C_{D,r}(\theta) \cdot a_R} \right)^2$

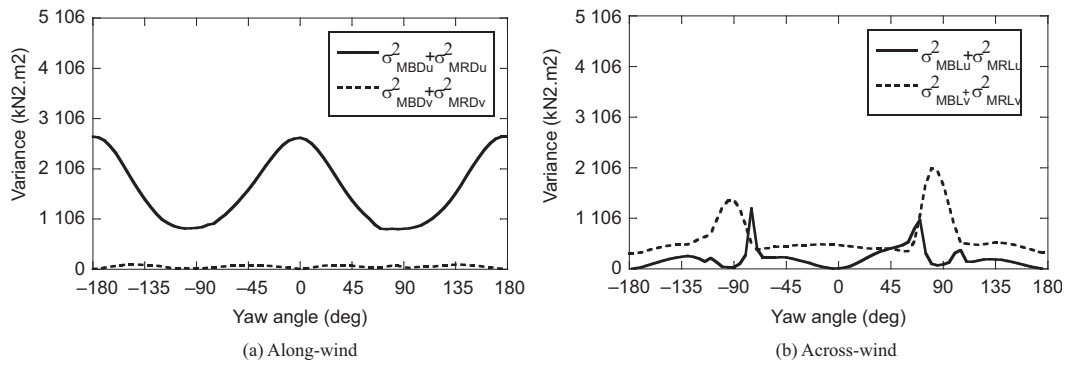


Figure 11. Comparison of standard deviation from u and v (400kW, $T_{th} = 0.158$)

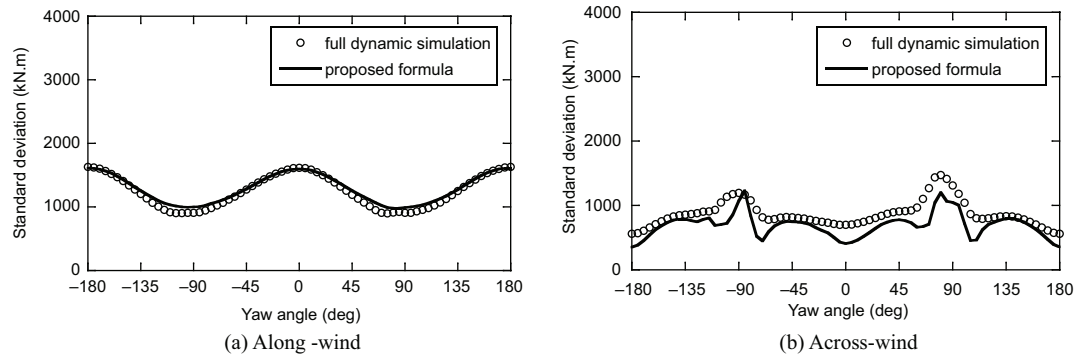


Figure 12. Comparison of tower base standard deviation for different yaw angles

Figs. 12 and 13 show that the proposed formulae of standard deviation correlate well with the full dynamic simulation for different yaw angles and different heights on tower. From Fig. 13, it is noticed that in across-wind load the standard deviation becomes maximum near $\pm 90^\circ$ resulted in the large gradient of aerodynamic coefficient $A_L(\theta)$ of rotor and show minimum value near 0° and $\pm 180^\circ$, just opposite to the situation of along-wind load. This is why the across-wind load should be considered when the inflow angle increases, and can be neglected compared to the along-wind load around 0° and $\pm 180^\circ$.

3.3. Peak factor

A study by Kareem and Zhou[16] proved that the bending moment-based peak factor can yield more reliable results than displacement-based peak factor, because the mean value of displacement may be zero. In order to take the non-linear component of wind load into account, Kareem et al. [17] evaluated the peak factor for the non-Gaussian process by employing the moment-based Hermite transformation which has been shown to be accurate and robust in representing the tail regions of the PDF in a non-Gaussian process. It is a function of kurtosis α_4 and skewness α_3 . Binh et al. [4] proved that the effect of kurtosis α_4 can be neglected since it is negligibly small compared to that

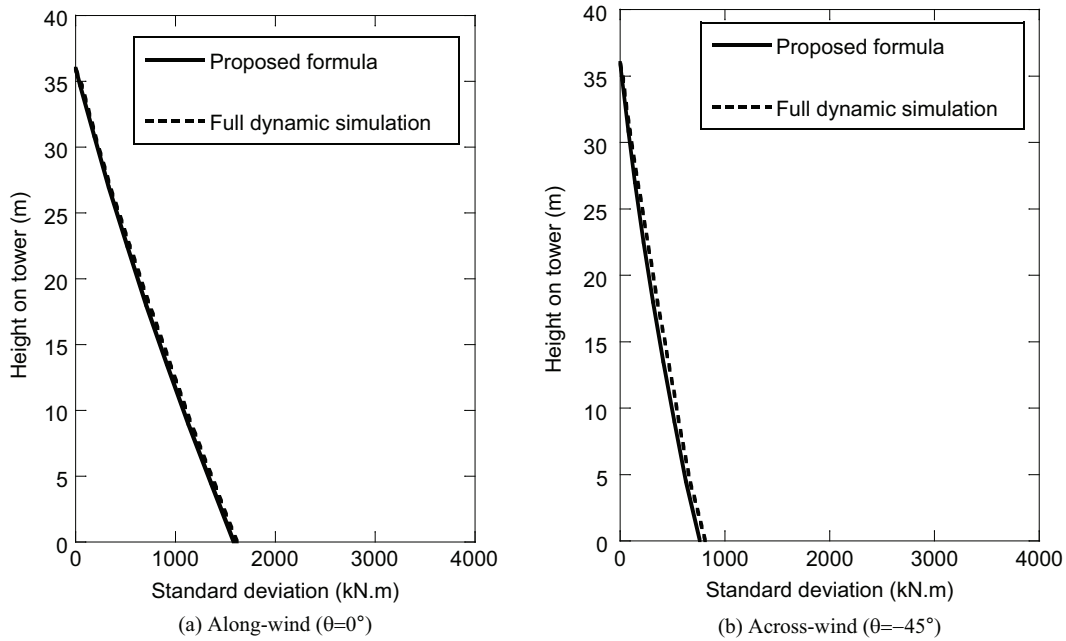


Figure 13. Comparison of standard deviation for different heights on tower

of the second and third order from the order analysis of turbulence intensity $I_u \cdot \alpha_4$ is then assumed to be equal to the value of a Gaussian process (i.e., 3.0). Then the formula of the peak factor is simplified to a function of skewness α_3 , as shown in eqn (17).

$$g_D = \frac{1}{\sqrt{1 + \frac{\alpha_3^2}{18}}} \left\{ \left(\sqrt{2 \ln(v'_D T)} + \frac{0.5772}{\sqrt{2 \ln(v'_D T)}} \right) + \frac{\alpha_3}{6} (2 \ln(v'_D T) + 0.1544) \right\} \quad (17)$$

where $v'_D = v_D / v'_D = v_D / \sqrt{(1 + \alpha_3^2 / 18)(1 + \alpha_3^2 / 9)}$ is the zero up-crossing number in the estimated time interval T (normally 600s) of non-Gaussian process.

$$v_D = n_1 \sqrt{\frac{(n_{0D} / n_1)^2 + R_D}{1 + R_D}}, \quad n_{0D} = 0.3 \frac{U_h}{\sqrt{L_u \sqrt{A_{wt}}}}$$

v'_D and v_D are the zero up-crossing number in the estimated time interval T (normally 600s) of non-Gaussian process and Gaussian process of along-wind load, respectively, A_{wt} is the wind acting area of the whole wind turbine.

Binh et al. [4] proposed a formula of skewness α_3 for wind turbines, considering both significant resonant response and spatial correlation of wind velocity using a correlation coefficient $\rho(r, r') = \exp[-|r - r'| / 0.3L_u]$.

$$\alpha_3 = \frac{1}{1.3R_D + 1} \times \frac{3I_{uh} a_{r1D}}{(K_{MBDu})^{\frac{3}{2}}} \quad (18)$$

where

$$R_D = \left(\frac{\sigma_{MRD}}{\sigma_{MBD}} \right)^2,$$

$$a_{r1D} = \frac{\iiint \rho(r, r') \rho(r', r'') C_D(r, \theta) C_D(r', \theta) C_D(r'', \theta) c(r) c(r') c(r'') r r' r'' dr dr' dr''}{\left(\int C_D(r, \theta) c(r) r dr \right)^3} \approx \frac{1}{1 + \beta_{1D} \frac{R}{0.3L_u}}$$

R_D is denoted the resonance-background ratio of along-wind standard deviation, and a_{r1D} is a size reduction factor, considering the lack of correlation of the fluctuating wind velocity. Since a_{r1D} is related to the background response, it can be formulated with the same analysis and approach as those of K_{MBDu} or K_{MBLDu} , and the unknown factor $\beta_{1D} = 1.67$ is proposed, which agrees well with its integral form, as shown in Fig. 14.

It is noticed from the full dynamic simulation that for the across-wind response, since the skewness and kurtosis of fluctuating wind load are close to 0 and 3.0, respectively, the non-Gaussian peak factor of eqn (17) can be reduced to the standard Gaussian form:

$$g_L = \sqrt{2 \ln(v_L T)} + \frac{0.5772}{\sqrt{2 \ln(v_L T)}} \tag{19}$$

where $v_L = n_1 \sqrt{\frac{(n_{0L}/n_1)^2 + R_L}{1 + R_L}}$, $n_{0L} = 0.3 \frac{U_h}{\sqrt{L_v} \sqrt{A_{wt}}}$, $R_L = \left(\frac{\sigma_{MRL}}{\sigma_{MBL}}\right)^2$.

v_L is the zero up-crossing number in the estimated time interval T (normally 600s) of Gaussian process of across-wind load.

The peak factors change very little with the wind direction and assumed constant along the tower. Fig. 15 shows the peak factor for $\theta = 0^\circ$ from proposed formulae and full dynamic simulation. It is noticed that the non-Gaussian peak factor increases when the turbulence intensity increases, while Gaussian peak factor keeps constant and lower value, which means a non-Gaussian peak factor is necessary for along-wind load especially in the high turbulence intensity, while a Gaussian peak factor is acceptable for across-wind load.

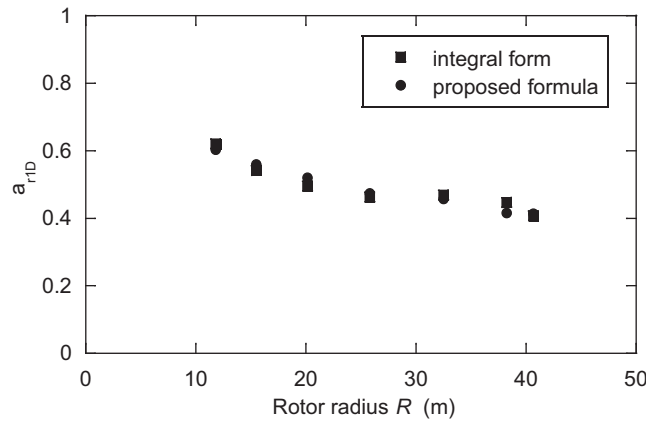


Figure 14. Size reduction factor a_{r1D}

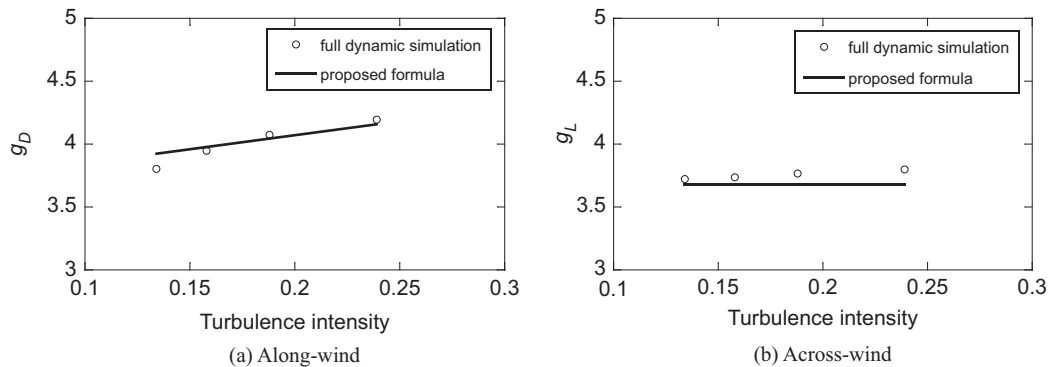


Figure 15. Comparison of peak factor for different turbulence intensity ($\alpha = 0^\circ$)

3.4. Combination of wind loads

Since the lift force on rotor becomes significant due to the increase of inflow angle, the combination of along-wind and across-wind loads is necessary for the estimation of design wind load on wind turbine towers. Coupled vibration can result from the small anisotropy of the tower, as shown in Fig. 16. It is noticed that the maximum values of along-wind and across-wind loads cannot appear simultaneously. Hence, their correlation coefficient should be considered.

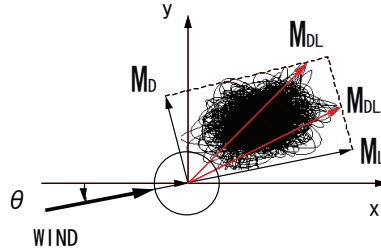


Figure 16. Tower bending moments plotted in X-Y plane

Asami[18] proposed a formula of wind loads combination for high-rise buildings, in which the across-wind bending moment combined with the maximum along-wind bending moment can be express as, $M_{LC} = \bar{M}_L + (\sqrt{2 + 2\rho_{DL}} - 1)(M_L - \bar{M}_L)$ where ρ_{DL} is the correlation coefficient between along wind and across wind responses. For the uncorrelated case ($\rho_{DL} = 0$), the coefficient multiplied to the maximum fluctuating component is 0.4 approximately, while for the completely correlated case ($\rho_{DL} = 1$), this coefficient becomes 1. In the same way, the along-wind bending moment combined with the maximum across-wind bending moment can be express as $M_{DC} = \bar{M}_D + (\sqrt{2 + 2\rho_{DL}} - 1)(M_D - \bar{M}_D)$. Finally, therefore, the maximum wind bending moment acting on the tower can be estimated as

$$M_{DL} = \max \left\{ \sqrt{M_L^2 + (\bar{M}_D + \gamma_{DL}(M_D - \bar{M}_D))^2}, \sqrt{M_D^2 + (\bar{M}_L + \gamma_{DL}(M_L - \bar{M}_L))^2} \right\} \quad (20)$$

where $\gamma_{DL} = \sqrt{2 + 2\rho_{DL}} - 1$. Fig. 17 shows the comparison of combined maximum bending moment on the tower base. It is noticed that the uncorrelated approximation ($\rho_{DL} = 0$) underestimates the maximum bending moment compared to the full dynamic simulation, while completely correlated approximation ($\rho_{DL} = 1$) can give a reasonable and conservative result. Therefore, $M_{DL} = \sqrt{M_D^2 + M_L^2}$ can be taken as a simpler alternative in the design.

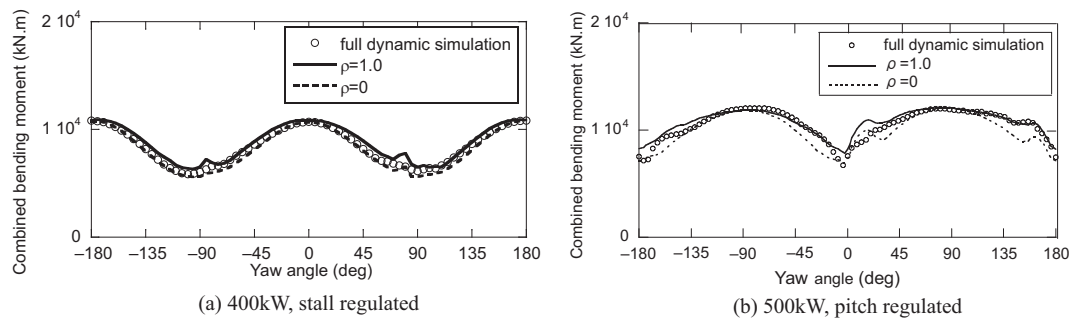


Figure 17. Comparison of combined maximum bending moment on tower base

CONCLUSIONS

In this study, the analytical formulae of the mean value, standard deviation and peak factor of both along-wind and across-wind loads are proposed based on the quasi-steady analysis as well as the formulae for the loads combination. The following conclusions are obtained:

- 1) The analytical formulae are proposed for not only along-wind but also across-wind mean bending moments, and agree well with the full dynamic simulation.

- 2) The mode correction factors, aerodynamic damping ratios and wind load ratios vary with the yaw angle due to the existence of rotor, while the size reduction factors keep almost constant with the different yaw angles, because the aerodynamic coefficients of the rotor are included in the numerator and denominator of the integral forms and do not contribute to the size reduction factors.
- 3) A non-Gaussian peak factor is necessary for the along-wind load, while a Gaussian peak factor is acceptable for the across-wind load.
- 4) The formula for the combination of along-wind and across-wind loads is derived. It is noticed that the completely correlated approximation can give a reasonable and conservative loading, while the uncorrelated approximation causes an underestimation.

APPENDIX

This appendix presents how the analytical formulae for standard deviations of bending moments are derived in detail.

A.1. Background response of base bending moment

From eqns (11–12), the background response of base bending moment can be expressed as eqn (A.1) in general.

$$M_{Bf}(t) = \int q_f(r, t) r dr = \int \rho c(r) C_f(r, \theta) U(r) u(r, t) r dr + \int \rho c(r) A_f(r, \theta) U(r) v(r, t) r dr \quad (\text{A.1})$$

where the subscript $f = D$ means along-wind and $f = L$ means across-wind.

Assuming that the cross correlation function of u, v components is zero, the standard deviation of background base bending moment can be derived as the summation of two independent parts due to longitudinal and lateral wind component (u and v) as well. Here, the mean wind velocity and turbulence intensity at the hub are also taken as representative for that of the whole wind turbine.

$$\begin{aligned} \sigma_{MBf}^2 &= \rho^2 \iint \rho_u(r, r') \sigma_u(r) \sigma_u(r') C_f(r) C_f(r') U(r) U(r') c(r) c(r') r r' dr dr' \\ &\quad + \rho^2 \iint \rho_v(r, r') \sigma_v(r) \sigma_v(r') A_f(r) A_f(r') U(r) U(r') c(r) c(r') r r' dr dr' \\ &\approx \rho^2 I_{uh}^2 U_h^4 \iint \rho_u(r, r') C_f(r) C_f(r') c(r) c(r') r r' dr dr' \\ &\quad + \rho^2 I_{vh}^2 U_h^4 \iint \rho_v(r, r') A_f(r) A_f(r') c(r) c(r') r r' dr dr' \\ &= \sigma_{MBfu}^2 + \sigma_{MBfv}^2 \end{aligned} \quad (\text{A.2})$$

where $\rho_u(r, r')$, $\rho_v(r, r')$ are the normalized cross correlation function between simultaneous wind fluctuation at r, r' , and measurements indicate that the normalized cross correlation function decays exponentially, so it can be expressed as $\rho_u(r, r') = \exp[-|r - r'|/0.3L_u]$ and $\rho_v(r, r') = \exp[-|r - r'|/0.3L_v]$. For design purpose, the background standard deviation can be expressed with mean bending moment, size reduction factor and wind load ratio. For wind turbine, the across-wind mean bending moment becomes close to zero at some yaw angles. And it is well known that the lateral turbulence intensity is defined as the ratio of standard deviation of lateral fluctuation component to the longitudinal mean wind speed. Based on the same idea, therefore, in this study the along-wind mean bending moment is employed to calculate both along-wind and across-wind standard deviation of bending moment. Therefore, the background standard deviation can be expressed as:

$$\sigma_{MBfu}(z) = 2 \frac{\bar{M}_D(z)}{1 + I_{uh}^2} I_{uh} \sqrt{K_{MBfu} \cdot \gamma_{MBfu}}, \quad \sigma_{MBfv}(z) = 2 \frac{\bar{M}_D(z)}{1 + I_{uh}^2} I_{vh} \sqrt{K_{MBfv} \cdot \gamma_{MBfv}} \quad (\text{A.3})$$

Where K_{MBfu} and K_{MBfv} are the background size reduction factors due to longitudinal and lateral wind fluctuations, respectively, as shown in eqns (A.4–A.5); γ_{MBfu} and γ_{MBfv} are wind load ratios, as shown in eqn (A.6).

$$K_{MBfu} = \frac{\iint \exp[-|r - r'|/0.3L_u] C_f(r, \theta) C_f(r', \theta) c(r) c(r') r r' dr dr'}{\left(\int C_f(r, \theta) c(r) r dr \right)^2} \quad (\text{A.4})$$

$$K_{MBfv} = \frac{\iint \exp[-|r-r'|/0.3L_v] A_f(r, \theta) A_f(r', \theta) c(r) c(r') rr' dr dr'}{\left(\int A_f(r, \theta) c(r) r dr\right)^2} \quad (A.5)$$

$$\gamma_{MBfu} = \frac{\left(\int C_f(r, \theta) c(r) r dr\right)^2}{\left(\int C_D(r, \theta) c(r) r dr\right)^2}, \quad \gamma_{MBfv} = \frac{\left(\int A_f(r, \theta) c(r) r dr\right)^2}{\left(\int C_D(r, \theta) c(r) r dr\right)^2} \quad (A.6)$$

A.2. Resonant response of base bending moment

Substitute the fluctuating wind load of eqns (11–12) to the modal equations of motion for along-wind and across-wind responses:

$$m_i \ddot{f}_i(t) + \left(c_i + \int \rho C_D U c(r) \mu_i^2(r) dr\right) \dot{f}_i(t) + m_i \omega_i^2 f_i(t) = \int [\rho C_D c(r) U u + \rho A_D c(r) U v] \mu_i(r) dr,$$

$$m_i \ddot{f}_i(t) + \left(c_i + \int \rho A_L U c(r) \mu_i^2(r) dr\right) \dot{f}_i(t) + m_i \omega_i^2 f_i(t) = \int [\rho C_L c(r) U u + \rho A_L c(r) U v] \mu_i(r) dr \quad (A.7)$$

Where m_i is the generalized mass, c_i is the generalized damping and w_i is the modal natural frequency in radians per second, $f_i(t)$ is the tip displacement, $\mu_i(r)$ is the normalized mode shape of the i th mode.

The generalized loading of the right hand side of eqn (A.7) can be expressed as eqn (A.8) in general with respect to the first mode.

$$Q_1(t) = \int \rho U(r) C_f(r, \theta) u(r, t) c(r) \mu_1(r) dr + \int \rho U(r) A_f(r, \theta) v(r, t) c(r) \mu_1(r) dr \quad (A.8)$$

Assuming that the cross correlation function of u, v components is zero, the standard deviation σ_{Q1} of $Q_1(t)$ is given by

$$\begin{aligned} \sigma_{Q1}^2 &= \frac{1}{T} \int_0^T Q_1^2(t) dt \\ &= \rho^2 \iint \left[\frac{1}{T} \int_0^T u(r, t) u(r', t) dt \right] U(r) U(r') C_f(r, \theta) C_f(r', \theta) c(r) c(r') \mu_1(r) \mu_1(r') dr dr' \\ &\quad + \rho^2 \iint \left[\frac{1}{T} \int_0^T v(r, t) v(r', t) dt \right] U(r) U(r') A_f(r, \theta) A_f(r', \theta) c(r) c(r') \mu_1(r) \mu_1(r') dr dr' \\ &\quad + 2\rho^2 \iint \left[\frac{1}{T} \int_0^T u(r, t) v(r', t) dt \right] U(r) U(r') C_f(r, \theta) A_f(r', \theta) c(r) c(r') \mu_1(r) \mu_1(r') dr dr' \\ &\approx \rho^2 \iint \left[\int_0^\infty S_{uu}(r, r', n) dn \right] U(r) U(r') C_f(r, \theta) C_f(r', \theta) c(r) c(r') \mu_1(r) \mu_1(r') dr dr' \\ &\quad + \rho^2 \iint \left[\int_0^\infty S_{vv}(r, r', n) dn \right] U(r) U(r') A_f(r, \theta) A_f(r', \theta) c(r) c(r') \mu_1(r) \mu_1(r') dr dr' \quad (A.9) \end{aligned}$$

where S_{uu}, S_{vv} is the cross spectrum of wind fluctuating component u, v respectively, which is defined by normalized co-spectrum $\psi_{uu}^N(r, r', n)$, $\psi_{vv}^N(r, r', n)$ and power spectrum density of its wind fluctuations $S_u(n), S_v(n)$.

$$S_{uu}(r, r', n) = \psi_{uu}^N(r, r', n) S_u(n), \quad S_{vv}(r, r', n) = \psi_{vv}^N(r, r', n) S_v(n)$$

Therefore, the power spectrum of generalized load with respect to the first mode is

$$S_{Q1}(n) = \rho^2 \iint \psi_{uu}^N(r, r', n) S_u(n) U(r) U(r') C_f(r, \theta) C_f(r', \theta) c(r) c(r') \mu_1(r) \mu_1(r') dr dr' \\ + \rho^2 \iint \psi_{vv}^N(r, r', n) S_v(n) U(r) U(r') A_f(r, \theta) A_f(r', \theta) c(r) c(r') \mu_1(r) \mu_1(r') dr dr' \quad (A.10)$$

As derived by Wind Energy Handbook[3], in the case of the dominant first mode, the power spectrum of the tip deflection is $S_{x1}(n) = S_{Q1}(n) |H_1(n)|^2$, where $S_{Q1}(n)$ is assumed constant over the narrow band of frequencies straddling the resonant frequency, $|H_1(n)|$ is the modulus of the

complex frequency response function, and can be used to transform the power spectrum of the wind incident into the power spectrum of the displacement. It has been shown by Newland[19] that $\int_0^\infty |H_1(n)|^2 dn = (\pi^2 / 2\delta_f) (n_1 / k_1^2)$. Then the standard deviation of resonant response becomes which can be written in two independence parts of longitude and lateral wind component (u and v).

$$\begin{aligned} \sigma_{x1}^2 &= \int_0^\infty S_{x1}(n) dn = \int_0^\infty S_{Q1}(n) |H_1(n)|^2 dn \approx S_{Q1}(n_1) \int_0^\infty |H_1(n)|^2 dn = S_{Q1}(n_1) \frac{\pi^2}{2\delta_f} \frac{n_1}{k_1^2} \\ &= \left[\frac{\pi^2}{2\delta_f} \frac{\rho^2}{k_1^2} \right] R_{uh}(n_1) I_{uh}^2 U_h^2 \iint \psi_{uu}(r, r', n_1) U(r) U(r') C_f(r, \theta) C_f(r', \theta) c(r) c(r') \mu_1(r) \mu_1(r') dr dr' \\ &\quad + \left[\frac{\pi^2}{2\delta_f} \frac{\rho^2}{k_1^2} \right] R_{vh}(n_1) I_{vh}^2 U_h^2 \iint \psi_{vv}(r, r', n_1) U(r) U(r') A_f(r, \theta) A_f(r', \theta) c(r) c(r') \mu_1(r) \mu_1(r') dr dr' \\ &= \sigma_{x1u}^2 + \sigma_{x1v}^2 \end{aligned} \quad (A.11)$$

Where δ_f is the logarithmic decrement of damping, which is 2π times the damping ratio ξ_f , $R_{uh}(n_1) = n_1 S_u(n_1) / \sigma_{uh}^2$ and $R_{vh}(n_1) = n_1 S_v(n_1) / \sigma_{vh}^2$ are the normalized power spectral density of longitudinal and lateral wind fluctuation.

The standard deviation of the first mode resonant base bending moment is derived below. Defining $M_{Rf}(t)$ as the fluctuating base bending moment due to wind excitation of the first mode

$$M_{Rf}(t) = \int m(r) \ddot{x}_1(t, r) r dr = \int m(r) \omega_1^2 x_1(t, r) r dr = \omega_1^2 f_1(t) \int m(r) \mu_1(r) r dr \quad (A.12)$$

Hence, based on eqns (A.11-A.12) the standard deviation of resonant base bending moment fluctuation can be derived as the summation of two independent parts resulted from longitudinal and lateral wind component (u and v) as well. Here, the mean wind velocity $U(r)$ and $U(r')$ in the integrals are assumed constant as U_h at the hub.

$$\begin{aligned} \sigma_{MRf}^2 &= \omega_1^4 (\sigma_{x1u}^2 + \sigma_{x1v}^2) \left(\int m(r) \mu_1(r) r dr \right)^2 = \sigma_{MRfu}^2 + \sigma_{MRfv}^2 \\ \sigma_{MRfu}^2 &= \omega_1^4 \sigma_{x1u}^2 \left(\int m(r) \mu_1(r) r dr \right)^2 \\ &= \frac{k_1^2}{m_1^2} \left[\frac{\pi^2}{2\delta_f} \frac{\rho^2}{k_1^2} \right] R_{uh}(n_1) I_{uh}^2 U_h^4 \iint \psi_{uu}(r, r', n_1) C_f(r, \theta) C_f(r', \theta) c(r) c(r') \mu_1(r) \mu_1(r') dr dr' \\ &\quad \cdot \left(\int m(r) \mu_1(r) r dr \right)^2 \\ \sigma_{MRfv}^2 &= \omega_1^4 \sigma_{x1v}^2 \left(\int m(r) \mu_1(r) r dr \right)^2 \\ &= \frac{k_1^2}{m_1^2} \left[\frac{\pi^2}{2\delta_f} \frac{\rho^2}{k_1^2} \right] R_{vh}(n_1) I_{vh}^2 U_h^4 \iint \psi_{vv}(r, r', n_1) A_f(r, \theta) A_f(r', \theta) c(r) c(r') \mu_1(r) \mu_1(r') dr dr' \\ &\quad \cdot \left(\int m(r) \mu_1(r) r dr \right)^2 \end{aligned} \quad (A.13)$$

On an empirical basis, Davenport[20] has proposed an exponential expression for the normalized co-spectrum as $\psi_{uu}^N(r, r', n) = \psi_{vv}^N(r, r', n) \approx \exp[-C|r - r'|n/U_h]$. Based on the same analysis, the resonant standard deviation can be expressed with along-wind mean bending moment, mode correction factor, size reduction factor and wind load ratio:

$$\begin{aligned} \sigma_{MRfu}(z) &= 2 \frac{\bar{M}_D(z)}{1 + I_{uh}^2} I_{uh} \frac{\pi \phi_f}{\sqrt{4\pi \xi_f}} \sqrt{R_{uh}(n_1)} \sqrt{K_{MRfu}(n_1) \cdot \gamma_{MRfu}} \\ \sigma_{MRfv}(z) &= 2 \frac{\bar{M}_D(z)}{1 + I_{vh}^2} I_{vh} \frac{\pi \phi_f}{\sqrt{4\pi \xi_f}} \sqrt{R_{vh}(n_1)} \sqrt{K_{MRfv}(n_1) \cdot \gamma_{MRfv}} \end{aligned} \quad (A.14)$$

where ϕ_f is the mode correction factor, ξ_f is the damping ratio, $K_{MRfu}(n_1)$ and $K_{MRfv}(n_1)$ are denoted the resonant size reduction factors due to longitudinal and lateral wind fluctuations, respectively, as shown in eqns (A.15-A.16); γ_{MRfu} and γ_{MRfv} are wind load ratios, as shown in eqn (A.17).

$$K_{MRfu}(n_1) = \frac{\iint \exp[-C|r-r'|n_1/U_h] C_f(r,\theta)C_f(r',\theta)c(r)c(r')\mu_1(r)\mu_1(r')dr dr'}{\left(\int C_f(r,\theta)c(r)\mu_1(r)dr\right)^2} \quad (\text{A.15})$$

$$K_{MRfv}(n_1) = \frac{\iint \exp[-C|r-r'|n_1/U_h] A_f(r,\theta)A_f(r',\theta)c(r)c(r')\mu_1(r)\mu_1(r')dr dr'}{\left(\int A_f(r,\theta)c(r)\mu_1(r)dr\right)^2} \quad (\text{A.16})$$

$$\gamma_{MRfu} = \frac{\left(\int C_f(r,\theta)c(r)\mu_1(r)dr\right)^2}{\left(\int C_D(r,\theta)c(r)\mu_1(r)dr\right)^2}, \quad \gamma_{MRfv} = \frac{\left(\int A_f(r,\theta)c(r)\mu_1(r)dr\right)^2}{\left(\int C_D(r,\theta)c(r)\mu_1(r)dr\right)^2} \quad (\text{A.17})$$

REFERENCES

- [1] IEC 61400-1, Wind turbines – Part 1: Design requirements, Ed.3, 2005.
- [2] ISO 4354, Wind actions on structures, 2005.
- [3] Burton, T., Sharpe, D., Jenkins, N., Bossanyi, E., *Wind energy handbook*. WILEY, England, 2001.
- [4] Binh, L.V., Ishihara, T., Phuc, P.V., Fujino, Y., A peak factor for non-Gaussian response analysis of wind turbine tower. *Journal of Wind Engineering and Industrial Aerodynamics* 96, 2217–2227, 2008.
- [5] Architectural Institute of Japan (AIJ), *Recommendations for loads on buildings*, 2004.
- [6] The Danish Society of Engineers and the Federation of Engineers, Loads and safety of wind turbine construction-Danish standard DS472, 1992.
- [7] Davenport, A.G., Note on the distribution of the largest value of a random function with application to gust loading. *In: Proceedings of the Institute of Civil Engineering*, pp. 187–196, 1964.
- [8] Ishihara, T., Guidelines for design of wind turbine support structures and foundations. *Japan Society of Civil Engineers*, Tokyo, 2010. (in Japanese)
- [9] Zhu, L., Seismic response of wind turbine in the parked and operating conditions, Ph.D dissertation, *Department of Civil Engineering*, University of Tokyo, Japan, 2007.
- [10] Ishihara, T., Phuc, P.V., Fujino, Y., Takahara, K., Mekaru, T., A field test and full dynamic simulation on a stall regulated wind turbine. *Proceedings of 6th Asia-Pacific Conference on Wind Engineering*, 599-612, 2005.
- [11] GH Bladed, Generic 2MW Offshore Turbine, GH Bladed Version3.51, *Garrad Hassan and Partners Limited*, 2001.
- [12] Somers, D.M., Design and Experimental Results for the S809 Airfoil, NREL/SR-6918, Golden, Colorado, National Renewable Energy Lab, 1997.
- [13] British Standards Institute: *Code of basic data for the design of buildings*, Chapter V, Loading.
- [14] Von Karman, T., Progress in the statistical theory of turbulence. *Journal of Maritime Research*, 7, 1948.
- [15] Cramer, H. E., Use of power spectra and scales of turbulence in estimating wind loads. Second National Conference on Applied Meteorology, Ann Arbor, Michigan, USA, 1958.
- [16] Kareem, A., Zhou, Y., Gust loading factor—past, present and future. *Journal of Wind Engineering and Industrial Aerodynamics* 91, 1301–1328, 2003.
- [17] Kareem, A., Tognarelli, M.A., Gurley, K.R., Modeling and analysis of quadratic term in the wind effects on structures. *Journal of Wind Engineering and Industrial Aerodynamics* 74–76, 1101–1110, 1998.
- [18] Asami, Y., Wind loads combination for high-rise building. *16th Symposium on Wind Engineering*, 531–534, 2000. (in Japanese)
- [19] Newland, D. E., Random vibrations and spectral analysis. Longman, UK, 1984.
- [20] Davenport, A. G., The response of slender, line-like structures to a gusty wind. *Proc. Inst. Civ. Eng.*, 23, 389–408, 1962.